City Research Online

City St George's, University of London

Citation: Bashir, M. N., Saad, H. M., Rizwan, M., Quazi, M. M., Ali, M. M., Ahmed, A., Zaidi, A. A., Soudagar, M. E. M., Haseeb, A. S. M. A. & Naher, S. (2022). Effects of tin particles addition on structural and mechanical properties of eutectic Sn–58Bi solder joint. Journal of Materials Science: Materials in Electronics, 33(28), pp. 22499-22507. doi: 10.1007/s10854-022-09028-5

This is the accepted version of the paper.

This version of the publication may differ from the final published version. To cite this item please consult the publisher's version.

Permanent repository link: https://openaccess.city.ac.uk/id/eprint/28953/

Link to published version: https://doi.org/10.1007/s10854-022-09028-5

Copyright and Reuse: Copyright and Moral Rights remain with the author(s) and/or copyright holders. Copies of full items can be used for personal research or study, educational, or not-for-profit purposes without prior permission or charge, unless otherwise indicated, provided that the authors, title and full bibliographic details are credited, a hyperlink and/or URL is given for the original metadata page and the content is not changed in any way. For full details of reuse please refer to City Research Online policy.

City Research Online: http://openaccess.city.ac.uk/ publications@citystgeorges.ac.uk

Effects of Tin Particles Addition on Structural and Mechanical Properties of Eutectic Sn-58Bi Solder Joint

M. Nasir Bashir[1], Hafiz Muhammad Saad[2], Muhammad Rizwan[3], M. M. Quazi[4], Muhammad Mahmood Ali[5], Arslan Ahmed[6], Asad A. Zaidi[7], Manzoore Elahi M. Soudagar[8], A.S.M.A. Haseeb*[9], Sumsun Naher*[10].

1,2. National University of Sciences and Technology, Islamabad, Pakistan

3. Department of Metallurgical Engineering NEDUET, Pakistan

4. Faculty of Mechanical and Automotive Engineering Technology, Universiti Malaysia Pahang, 26600 Pekan, Pahang, Malaysia

5. Centre for Mathematical Modelling and Intelligent Systems for Health and Environment (MISHE), Atlantic Technological University Sligo, Ash Lane, F91 YW50 Sligo, Ireland

6. Department of Mechanical Engineering Comsats University Islamabad, Wah campus, Wah Cantt, Pakistan

7. Department of Mechanical Engineering, Faculty of Engineering Sciences and Technology, Hamdard University, 74600 Karachi, Pakistan

8. University Centre for Research & Development, Department of Mechanical Engineering, Chandigarh University, Mohali, 140413, Punjab, India

9. Department of Mechanical Engineering, University of Malaya, Kuala Lumpur, 50603, Malaysia

10. Department of Mechanical Engineering and Aeronautics, City, University of London, London, United Kingdom

Email of Corresponding Author: haseeb@um.edu.my
sumsun.naher.1@city.ac.uk

Abstract:

Due to the inherent environmental and health toxicities associated with lead, the use of environmental friendly lead-free solder materials has become an unavoidable trend in the electronic packaging industry. Sn-58Bi alloy is gaining attention for its good material properties such as low melting point, reliability and high tensile strength. The presence of the bismuth-rich phase increases the brittleness of Sn-58Bi alloy. The purpose of this study is to suppress the brittleness of Sn-58Bi alloy by the addition of different wt% (0, 10, 20, 30) of Sn powder. The powder metallurgy method was used to prepare the samples. Scanning electron microscopy and energy dispersive X-ray analysis were done to study the structural properties and a tensile test was done by a universal tensile machine to study the mechanical properties. The results reveal that the Sn particles partially dissolved in the Sn-58Bi solder matrix. The dissolution of Sn particles significantly improved the mechanical strength by 30%, suppressed the brittleness and improved the strain value by 1.3 times.

Keywords: Sn powder, Sn-58Bi powder, Ductility, Tensile strength, Microstructure.

1. INTRODUCTION:

In the electronic packaging industry, eutectic or near eutectic Sn-Pb solder alloys are used to connect electronic components on printed circuit boards (PCBs) due to their low melting temperature, excellent material properties, and low cost [1, 2]. Due to the inherent environmental and health toxicities associated with lead, the use of environmental friendly lead-free solder materials has become an unavoidable trend in the electronic packaging industry [3, 4]. In this consequence, intensive research has been conducted over the last few decades to find suitable lead-free alloys that replace the use of lead-based alloys in the industry [5, 6].

There have been several Pb-Free solder materials found to substitute the Pb-based solder [1, 7]. The most popular of these is a tin-bismuth (Sn-Bi) solder alloy [8, 9]. Sn-Pb solder alloys have been replaced with Sn-Bi solder alloys as both solder alloys have the same mechanical properties at lower temperatures, and the melting point of the eutectic Sn-Bi alloys is much lower than that of the Sn-Pb alloys [10-12]. During the reflow process, the intermetallic compound (IMC) develops and contributes to the solder interface [13, 14]. The IMC's morphology varies with soldering conditions. As the homologous temperature rises, the diffusion rate of atoms in solder increases, resulting in an increase in the thickness of the IMC in the solder joint[15, 16]. Due to an increase in the thickness of the IMC, the solder joint may have reliability issues [17, 18].

Different types of studies have been done to find a way to increase the Sn-Bi solder alloy's reliability including adding alloying elements [19, 20], microparticles [21, 22], nanoparticles (NP) [23-27] and carbon nanotubes [28]. In the past, Ni [29], Sb [30], Cu and Zn [31] and Ag [32, 33] have been added to the Sn-Bi solder joint. Despite the promising properties enhancement by the addition of different reinforcement particles into Sn-Bi eutectic alloy, researchers have paid less attention to the effects of Sn added to Sn-Bi solder alloys. Tin is one of the potential candidates that can be added for increased reliability of the solder [34]. With the addition of Sn to form composite solder, it is expected that the brittleness of Sn-58Bi eutectic alloy can be suppressed by hindering the crack propagation with the embedment of Sn particles in the Sn-58Bi solder matrix [35].

Due to the brittleness of Bi rich phases, the crack will initiate and propagate easily when under external loading such as shear stress due to coefficient of thermal expansion (CTE) mismatch between 2 types of materials [36]. It is necessary to know the microstructure of the solder matrix and tensile properties after adding Sn to the system to understand the Sn-58Bi solder matrix. The major concern is the brittleness of eutectic Sn-58Bi solder alloy while processing electronic devices [37]. So, there is a need to understand the effect of Sn reinforcement particles on the microstructure and the mechanical properties of the eutectic Sn-58Bi solder matrix. Sn particles

must be able to distribute and embed inside the matrix and how wt% of Sn particles addition will affect the structural and mechanical properties of eutectic Sn-58Bi solder matrix.

This study investigates the effect of the addition of different wt% of Sn powder in eutectic Sn-58Bi solder matrix on the structure and mechanical properties. The Sn particles are ductile in nature while the Bi-phase present in Sn-58Bi solder is brittle. After the addition of Sn, the material properties such as ductility, mechanical strength and microstructure might be improved. Composite solder alloys were prepared using the powder metallurgy method and then samples were cross-sectioned to observe the microstructural changes by scanning electron microscope (SEM) analysis and energy dispersive x-ray (EDX) analysis was done to observe the distribution of Sn powder in the solder matrix. Then, tensile tests were conducted after reflow to study how Sn powder affects the tensile strength of the eutectic Sn-58Bi solder matrix.

2. METHODOLOGY:

Sample preparation for structure and mechanical properties via powder metallurgy method was prepared. The Sn powder was dried at 50^{o}C for 12 hours (h) to eliminate moisture. After that, 10, 20 and 30 wt% of Sn powder of size 25±2 μm were mixed with Sn-58Bi solder powder to obtain Sn and Sn-Bi powder mixture. The mixture was blended for 30 minutes manually to ensure thorough mixing. For structure properties, 0.9 g of powder mixture was placed between 2 pellets as shown in Fig. 1 (a) and pressed the powder mixture into disk shape structure sample of size 3 mm as shown in Fig 1 (b). The sample was then reflowed in the reflow oven. After the reflow, two sets of samples were prepared. One set of samples was for microstructure properties and the second set of samples was for tensile properties as shown in Fig 1 (c and e). For the first set of samples, the mounting process of samples by using epoxy resin and hardener was done. A mounting cup with an inner diameter of 30 mm was used. The samples were placed vertically into a mounting cup by using a plastic holder as shown in Figure 1 (d). After that, a mixture of epoxy resin and hardener was placed in the mounting cup. The mounting cup was kept in a room temperature for 6 h to solidify the mixture. After solidification, the samples were taken out from the mounting cup and were cross-sectioned and polished. A cross-sectional view of samples was observed through a scanning electron microscope (SEM). Energy dispersive X-ray (EDX) analysis was used to understand the distribution of Sn powder inside the Sn-58Bi solder matrix.

For the second set of samples, two copper bars with a dimension of 25 mm x 3 mm x 2 mm were taken. One end of the copper bars was cleaned to remove the oxidation layer. The cleaning process was done by using distilled water and 20% sulphuric acid (H_2SO_4). The samples were kept for 1 minute in a chemical solution. The solder

disk shown in Fig 1 (b) was placed between two copper bars as shown in Fig 1 (e) and then reflowed in the reflow oven. After the preparation of tensile samples via the powder metallurgy method, a tensile test was carried out by a universal tensile machine (UTM) (Model No. Instron 3382A). A strain rate of $6.96\times10^{-4}\ s^{-1}$ was applied to pull the samples as shown in Fig 1 (f).

3. RESULTS AND DISCUSSIONS:

3.1Microstructure after Reflow:

Sn-58Bi solder powder with the addition of different wt% of Sn powder was cross-sectioned. Scanning electron microscopy (SEM) and energy dispersive X-ray (EDX) spectroscopy were used to analyze the samples. Figure 2 (a) shows an SEM image of Sn-58Bi solder powder with 10 wt% of Sn powder addition after reflow. The selected points in the image show the compressed Sn particles. SEM image showed that Sn powder was distributed non-uniformly inside the eutectic Sn-58Bi solder matrix. Sn particles can be easily differentiated from the Sn-58Bi solder matrix. It was observed in Fig 2 (a) that the particles were trapped inside the Sn-58Bi solder matrix. Due to compression, the shape of the Sn particle was changed from spherical to the irregular shape. The Sn particles that were near the top surface of the solder bump, floated in the flux due to the lower density of Sn particles. The Sn particle was still in the solid-state and Sn-58Bi solder powder was in the molten form. Sn has a lower density than Sn-58Bi eutectic solder alloy. Sn has a density of $7.31\ g/cm^3$ and Sn-Bi eutectic alloy has a density of $8.12\ g/cm^3$. During the reflow process, when Sn-58Bi starts to melt and form a molten state, Sn particles will float to the surface due to bouncy force resulting from density difference [38]. An SEM image of floated Sn particle was shown in Fig 2 (b). The bonding strength between Sn particle and eutectic Sn-58Bi solder matrix is too weak [35] to retain Sn particles inside the matrix is another reason why Sn particle was unable to remain inside the Sn-58Bi solder matrix as shown in Fig 2 (b). Fig 2 (c) shows the EDX spectrum obtained from spot analysis performed at the selected point. This spectrum shows that Sn particles were present in the Sn-58Bi solder matrix. Sn particles had a higher concentration than Bismuth (Bi) at this point in Fig 2 (a). The samples were reflowed under low temperature and for a shorter time and the size of Sn particles were bigger. Due to this, the Sn particles dissolved partially. The reason was that the Sn particles were not able to completely dissolve within 90 seconds of the reflow process.

Figure 3 (a) shows an SEM image of eutectic Sn-58Bi solder powder with 20 wt% of Sn powder addition after reflow. The selected points in the image show the Sn particles. Sn particles were found in irregular shapes in the eutectic Sn-58Bi solder matrix. The distribution of Sn was non-uniform and the shape was irregular. Fig 3 (b)

shows the EDX analysis. The spot analysis was done. The EDX analysis revealed that a high concentration of Sn particles were found on the selected spot in Fig 3 (a). This conveyed the presence of Sn particles in the eutectic Sn-58Bi solder matrix.

Figure 4 (a) and (b) show the Sn-58Bi solder matrix with 0% and 30% Sn powder addition after reflow. When Sn powder was added to the Sn-58Bi solder matrix, Bi started to diffuse into Sn particle forming alloy as shown in Fig 4 (c and d). Similar results were found by Lee et al. [39]. They found that the Bi started to diffuse into Sn after plating. At 0% Sn addition, Sn rich phase and Bi rich phase tangled against each other to form a complete Sn-58Bi matrix. However, when extra Sn particles were added, Sn particles started to dissolve into the solder matrix forming equiaxed-shaped Sn particles as shown in Fig 4 (b). With the addition of Sn particle into Sn-58Bi solder powder, Bi diffused in Sn particles forming Sn-rich Sn-58Bi solder alloy in Figure 4 (c and d). This phenomenon is explained by the Ostwald Ripening process [40]. Sn particles are ductile and the Sn-58Bi solder matrix is brittle [41, 42]. Dissolution of Sn particles in Sn-58Bi solder matrix can participate to increase the ductility of Sn-58Bi solder. The material properties of Sn particles are higher than the Sn-58Bi solder matrix. So, the dissolution of Sn particle can participate in the improvement of material properties of Sn-58Bi solder matrix [43-45].

3.2 Tensile Test Analysis:

Figure 5 shows the Stress-Strain curves of Sn-58Bi at different wt% concentrations of Sn particles. Stress-strain curves were plotted for four sets of samples i.e. 0 wt%, 10 wt%, 20 wt% and 30 wt%. The average value of stress and strain are plotted in Fig 5. The result revealed that the eutectic Sn-58Bi solder matrix had the lowest stress and strain curves. After the addition of the Sn particles, the stress and strain curves increased. The ductility was improved by Sn powder addition due to an increase in the plasticity region as shown in Fig 5. The strain values also increased from 6.11±0.36 mm to 7.96±0.33 mm. The stress and strain values are tabulated in Table 1. The possible reason is that when extra Sn particles were added, Sn particles started to dissolve into the solder matrix forming equiaxed-shaped Sn particles as shown in Fig 4 (b). Sn particle which has higher hardness [46], higher tensile strength [47] and higher ductility [42] than Bi, which bridge the crack propagation causing more energy is required to further propagate the crack, hence ductility will be increased.

Figure 6 shows the Tensile strength of Sn-58Bi solder matrix at 0%, 10%, 20% and 30% wt% concentration of Sn powder. This figure shows that the Sn-58Bi solder matrix with the addition of 30% wt Sn powder has the highest tensile strength of 91.75 MPa as compared to the Sn-58Bi solder matrix without the addition of Sn

powder. The tensile strength of Sn-58Bi solder matrix with the addition of 10% and 20% wt Sn powder is 79.41 MPa and 84.82 MPa, respectively.

4. CONCLUSION:

The effect of the addition of Sn powder in Sn-58Bi solder matrix at different wt% concentrations on the structure and mechanical properties was investigated. Sn powder was added to Sn-58Bi powder and compressed. After reflow, the compressed Sn particles partially dissolved in the Sn-58Bi solder matrix. It was also observed that some Sn particles floated on the surface of the eutectic Sn-58Bi solder matrix due to lower density. The dissolved Sn particles improved the mechanical strength and ductility. In a higher concentration of Sn particle addition, the mechanical strength increased by 30% and the strain value increased by 1.3 times compared to Sn-58Bi solder.

5. Acknowledgment:

The financial support was provided by City, University of London, United Kingdom and University of Malaya, Kuala Lumpur, Malaysia.

6. Author Contributions:

All authors contributed equally.

7. Data Availability:

The current study is based on experimental data. In manuscript, the experimental data was correlated and discussed with existing studies done by other researchers (given in the references). The experimental data of current study is unpublished and will be provided for the evidences and for the review.

8. Compliance with Ethical Standards:

The authors followed the ethical standards during the experiments as well as for preparation of manuscript.

9. Competing Interests:

The authors have no relevant financial interests to disclose.

10.REFERENCES:

1. Kang, S.K. and A.K. Sarkhel, *Lead (Pb)-free solders for electronic packaging.* Journal of electronic materials, 1994. **23**(8): p. 701-707.
2. Yang, C., et al., *Recycling tin from electronic waste: a problem that needs more attention.* ACS Sustainable Chemistry & Engineering, 2017. **5**(11): p. 9586-9598.
3. Ringgaard, E. and T. Wurlitzer, *Lead-free piezoceramics based on alkali niobates.* Journal of the European Ceramic Society, 2005. **25**(12): p. 2701-2706.
4. Su, L.-H., et al., *Interfacial reactions in molten Sn/Cu and molten In/Cu couples.* Metallurgical and Materials Transactions B, 1997. **28**(5): p. 927-934.
5. Goosey, M., *An overview of the current status of lead-free assembly and related issues.* Circuit world, 2003.
6. Miric, A.Z. and A. Grusd, *Lead-free alloys.* Soldering & Surface Mount Technology, 1998.
7. Xu, L., et al., *Design and performance of Ag nanoparticle-modified graphene/SnAgCu lead-free solders.* Materials Science and Engineering: A, 2016. **667**: p. 87-96.
8. Bradley, E. *Lead-free solder assembly: impact and opportunity*. in *Electronic Components and Technology Conference*. 2003. IEEE; 1999.
9. Sahasrabudhe, S., et al. *Low Temperature Solder-A Breakthrough Technology for Surface Mounted Devices*. in *2018 IEEE 68th Electronic Components and Technology Conference (ECTC)*. 2018. IEEE.
10. Mei, Z. and J. Morris, *Characterization of eutectic Sn-Bi solder joints.* Journal of Electronic Materials, 1992. **21**(6): p. 599-607.
11. Gain, A.K. and L. Zhang, *Growth mechanism of intermetallic compound and mechanical properties of nickel (Ni) nanoparticle doped low melting temperature tin–bismuth (Sn–Bi) solder.* Journal of Materials Science: Materials in Electronics, 2016. **27**(1): p. 781-794.
12. Liu, Y. and K. Tu, *Low melting point solders based on Sn, Bi, and In elements.* Materials Today Advances, 2020. **8**: p. 100115.
13. Yin, C., et al., *The effect of reflow process on the contact resistance and reliability of anisotropic conductive film interconnection for flip chip on flex applications.* Microelectronics Reliability, 2003. **43**(4): p. 625-633.
14. Yu, C., et al., *First-principles investigation of the structural and electronic properties of Cu6−xNixSn5 (x= 0, 1, 2) intermetallic compounds.* Intermetallics, 2007. **15**(11): p. 1471-1478.
15. Nai, S., J. Wei, and M. Gupta, *Interfacial intermetallic growth and shear strength of lead-free composite solder joints.* Journal of Alloys and Compounds, 2009. **473**(1-2): p. 100-106.
16. Wang, Z., et al., *Influences of Ag and In alloying on Sn-Bi eutectic solder and SnBi/Cu solder joints.* Journal of Materials Science: Materials in Electronics, 2019. **30**(20): p. 18524-18538.
17. Chen, W.-H., et al., *IMC growth reaction and its effects on solder joint thermal cycling reliability of 3D chip stacking packaging.* Microelectronics Reliability, 2013. **53**(1): p. 30-40.
18. So, A.C. and Y.C. Chan, *Reliability studies of surface mount solder joints-effect of Cu-Sn intermetallic compounds.* IEEE Transactions on Components, Packaging, and Manufacturing Technology: Part B, 1996. **19**(3): p. 661-668.
19. Kotadia, H.R., P.D. Howes, and S.H. Mannan, *A review: On the development of low melting temperature Pb-free solders.* Microelectronics Reliability, 2014. **54**(6-7): p. 1253-1273.
20. Kamaruzzaman, L.S. and Y. Goh, *Effects of alloying element on mechanical properties of Sn-Bi solder alloys: a review.* Soldering & Surface Mount Technology, 2022.
21. Yao, P., P. Liu, and J. Liu, *Effects of multiple reflows on intermetallic morphology and shear strength of SnAgCu–xNi composite solder joints on electrolytic Ni/Au metallized substrate.* Journal of Alloys and Compounds, 2008. **462**(1-2): p. 73-79.
22. Ahmed, M., et al., *Influence of Ag micro-particle additions on the microstructure, hardness and tensile properties of Sn–9Zn binary eutectic solder alloy.* Microelectronics Reliability, 2010. **50**(8): p. 1134-1141.
23. Chang, S., et al., *Effect of addition of TiO2 nanoparticles on the microstructure, microhardness and interfacial reactions of Sn3. 5AgXCu solder.* Materials & Design, 2011. **32**(10): p. 4720-4727.
24. Bashir, M.N., et al., *Reduction of electromigration damage in SAC305 solder joints by adding Ni nanoparticles through flux doping.* Journal of materials science, 2015. **50**(20): p. 6748-6756.

25. Bashir, M.N., et al., *Effect of cobalt doping on the microstructure and tensile properties of lead free solder joint subjected to electromigration.* Journal of Materials Science & Technology, 2016. **32**(11): p. 1129-1136.
26. Bashir, M.N. and A. Haseeb, *Improving mechanical and electrical properties of Cu/SAC305/Cu solder joints under electromigration by using Ni nanoparticles doped flux.* Journal of Materials Science: Materials in Electronics, 2018. **29**(4): p. 3182-3188.
27. Bashir, M.N. and A. Haseeb, *Grain size stability of interfacial intermetallic compound in Ni and Co nanoparticle-doped SAC305 solder joints under electromigration.* Journal of Materials Science: Materials in Electronics, 2022: p. 1-9.
28. Nai, S., J. Wei, and M. Gupta, *Improving the performance of lead-free solder reinforced with multi-walled carbon nanotubes.* Materials Science and Engineering: A, 2006. **423**(1-2): p. 166-169.
29. Xu, G., et al., *Retarding the electromigration effects to the eutectic SnBi solder joints by micro-sized Ni-particles reinforcement approach.* Journal of alloys and compounds, 2011. **509**(3): p. 878-884.
30. Li, J.-G., et al. *Effects of Sb addition on the microstructure and mechanical performance of Sn58Bi based alloys and the solder joints*. in *2018 19th International Conference on Electronic Packaging Technology (ICEPT)*. 2018. IEEE.
31. Shen, J., et al., *Effects of minor Cu and Zn additions on the thermal, microstructure and tensile properties of Sn–Bi-based solder alloys.* Journal of Alloys and Compounds, 2014. **614**: p. 63-70.
32. Li, Y. and Y. Chan, *Effect of silver (Ag) nanoparticle size on the microstructure and mechanical properties of Sn58Bi–Ag composite solders.* Journal of Alloys and compounds, 2015. **645**: p. 566-576.
33. Liu, S., et al., *Effects of Ag on the microstructure and shear strength of rapidly solidified Sn–58Bi solder.* Journal of Materials Science: Materials in Electronics, 2019. **30**(7): p. 6701-6707.
34. Suganuma, K., *Advances in lead-free electronics soldering.* Current Opinion in Solid State and Materials Science, 2001. **5**(1): p. 55-64.
35. Kang, H., S.H. Rajendran, and J.P. Jung, *Low melting temperature Sn-Bi solder: Effect of alloying and nanoparticle addition on the microstructural, thermal, interfacial bonding, and mechanical characteristics.* Metals, 2021. **11**(2): p. 364.
36. Abtew, M. and G. Selvaduray, *Lead-free solders in microelectronics.* Materials Science and Engineering: R: Reports, 2000. **27**(5-6): p. 95-141.
37. Wang, J., et al. *Mechanical properties and joint reliability improvement of Sn-Bi alloy*. in *2011 IEEE 13th Electronics Packaging Technology Conference*. 2011. IEEE.
38. Wu, C., et al., *Properties of lead-free solder alloys with rare earth element additions.* Materials Science and Engineering: R: Reports, 2004. **44**(1): p. 1-44.
39. Lee, S.F., Y. Goh, and A. Haseeb. *Effects of stacking sequence of electrodeposited Sn and Bi layers on reflowed Sn-Bi solder alloys*. in *2012 35th IEEE/CPMT International Electronics Manufacturing Technology Conference (IEMT)*. 2012. IEEE.
40. Yec, C.C. and H.C. Zeng, *Synthesis of complex nanomaterials via Ostwald ripening.* Journal of Materials Chemistry A, 2014. **2**(14): p. 4843-4851.
41. Yang, L., et al., *Microstructure, IMCs layer and reliability of Sn-58Bi solder joint reinforced by Mo nanoparticles during thermal cycling.* Materials Characterization, 2019. **148**: p. 280-291.
42. Wang, Q., et al., *A micro-alloyed Mg-Sn-Y alloy with high ductility at room temperature.* Materials Science and Engineering: A, 2018. **735**: p. 131-144.
43. Liao, Y.-H., et al., *A comprehensive study of electromigration in pure Sn: Effects on crystallinity, microstructure, and electrical property.* Acta Materialia, 2020. **200**: p. 200-210.
44. Ye, D., et al., *Microstructure and mechanical properties of Sn–xBi solder alloy.* Journal of Materials Science: Materials in Electronics, 2015. **26**(6): p. 3629-3637.
45. Soares, D., et al., *The effect of Bi addition on the electrical and microstructural properties of SAC405 soldered structure.* Soldering & Surface Mount Technology, 2020. **33**(1): p. 19-25.
46. Liu, X., et al., *Melting behavior and the correlation of Sn distribution on hardness in a nanostructured Al–Sn alloy.* Materials Science and Engineering: A, 2009. **506**(1-2): p. 1-7.
47. Jin, S.-C., et al., *Improvement in tensile strength of extruded Mg–5Bi alloy through addition of Sn and its underlying strengthening mechanisms.* Journal of Magnesium and Alloys, 2021.

Figures

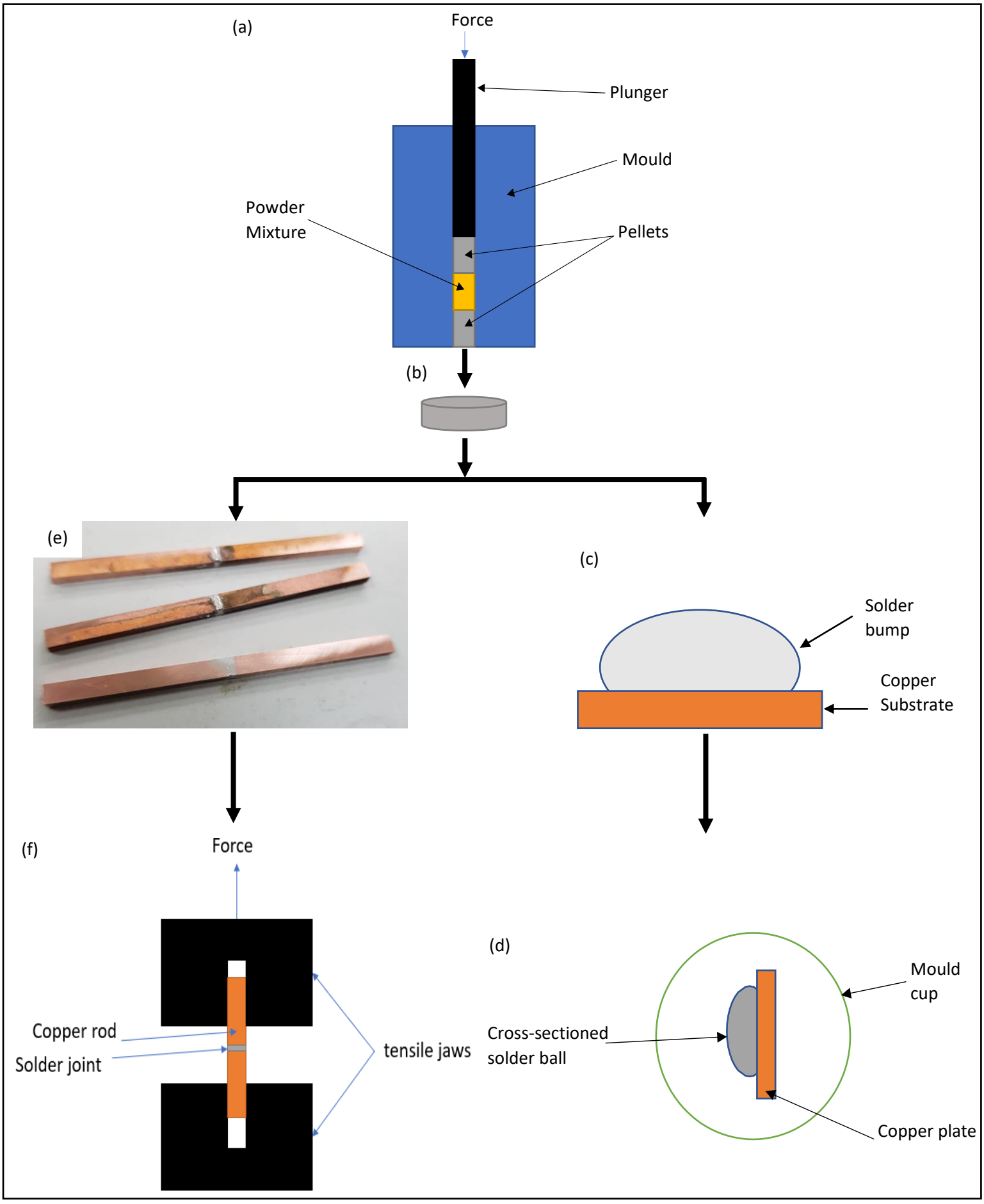

Figure 1 shows (a) Schematic of compression of powder mixture into pellet form, (b) Solder disk, (c) Solder bump after reflow, (d) Schematic of sample placed in mould cup to cross-section the sample for SEM, (e) Preparation of Tensile sample and (f) Schematic of tensile test of the samples.

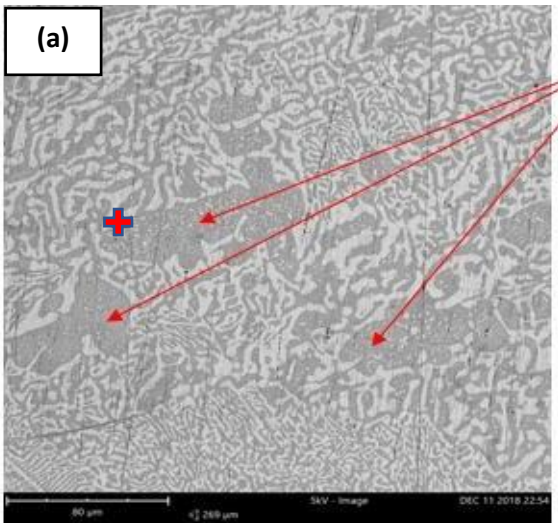

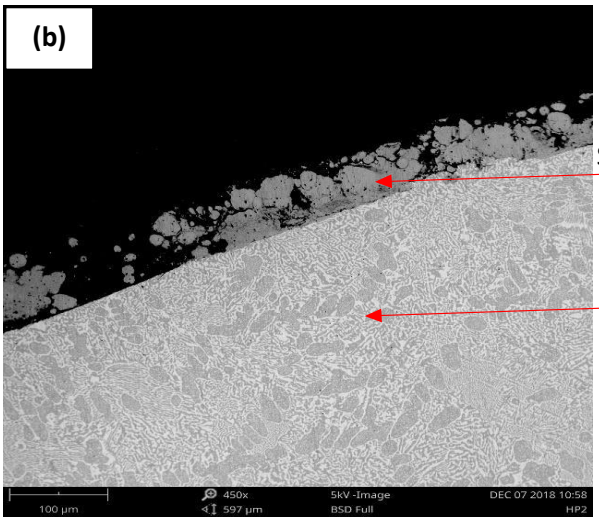

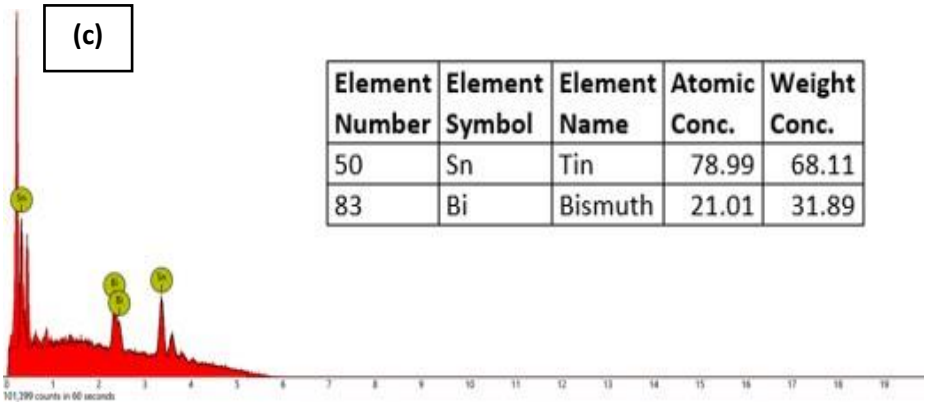

Element Number	Element Symbol	Element Name	Atomic Conc.	Weight Conc.
50	Sn	Tin	78.99	68.11
83	Bi	Bismuth	21.01	31.89

Figure 2 shows (a) SEM image of solder joint with 10wt% of Sn addition, (b) SEM image of floated and dissolved Sn particles and (c) EDX spectrum obtained from spot analysis performed at the selected point as labelled in (a).

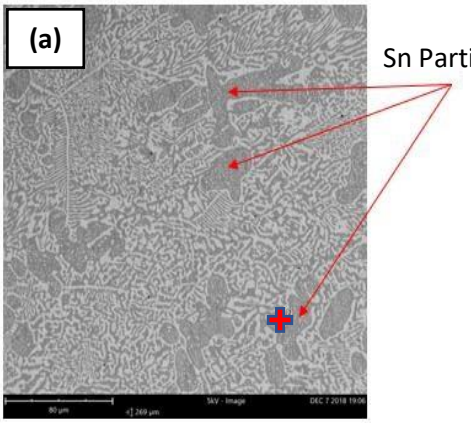

Sn Particles

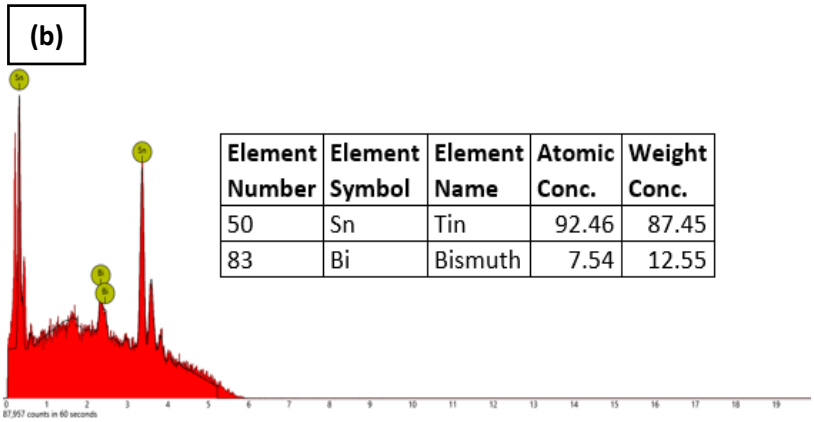

Element Number	Element Symbol	Element Name	Atomic Conc.	Weight Conc.
50	Sn	Tin	92.46	87.45
83	Bi	Bismuth	7.54	12.55

Figure 3 shows (a) SEM image of solder joint with 20wt% of Sn addition and (b) EDX spectrum obtained from spot analysis performed at the selected point as labelled in (a).

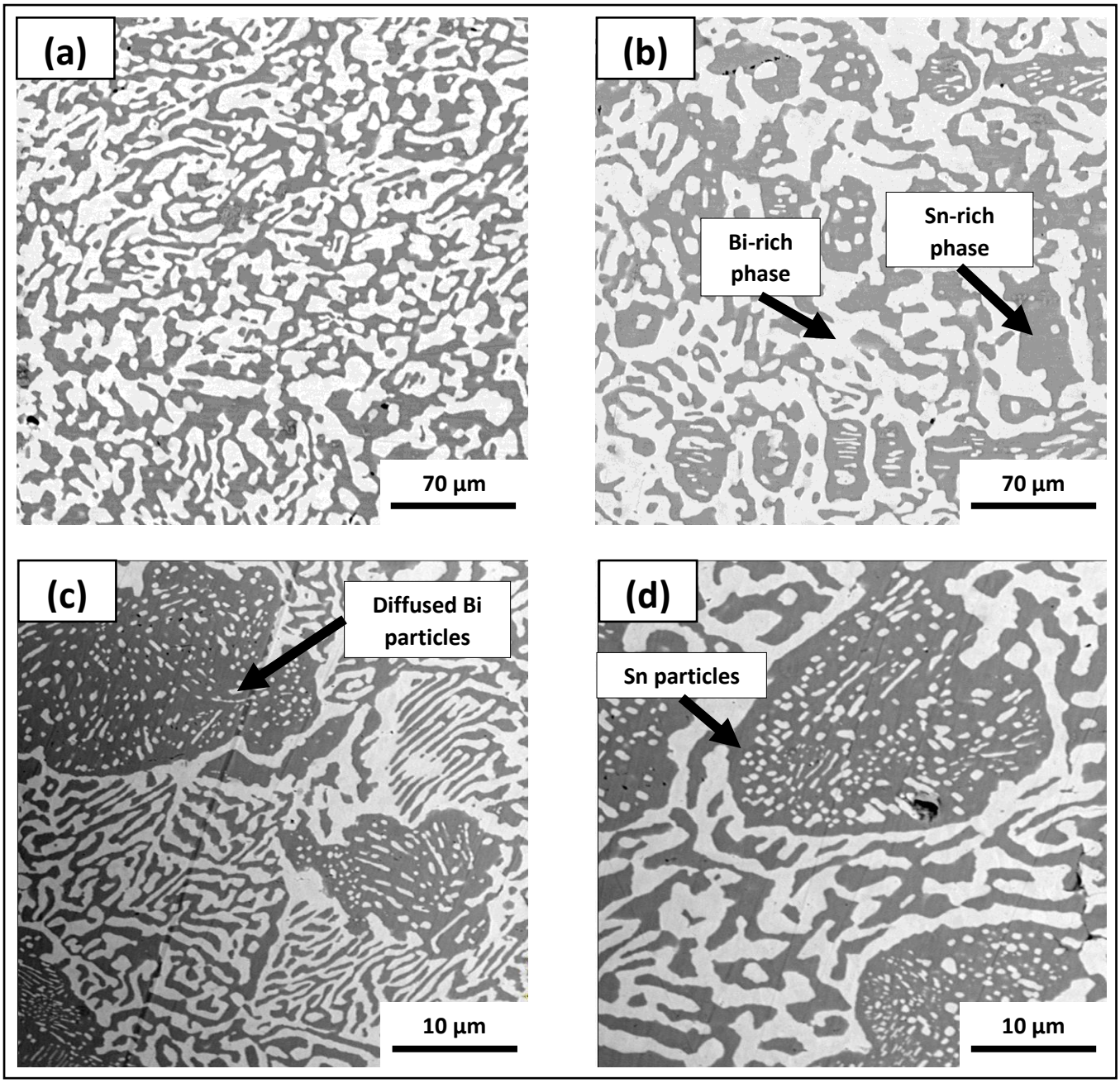

Figure 4 shows SEM images of Sn-58Bi with (a) 0% Sn addition (b) 30% Sn addition, (c) 20 wt% Sn addition with higher magnification and (d) 30% Sn addition with higher magnification.

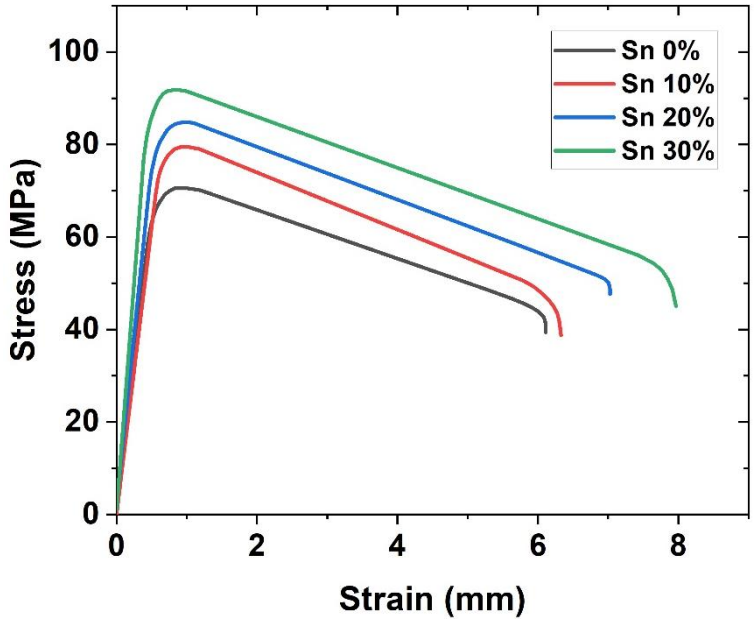

Figure 5 Stress-Strain curves of Sn-58Bi before and after addition of different wt% of Sn particles.

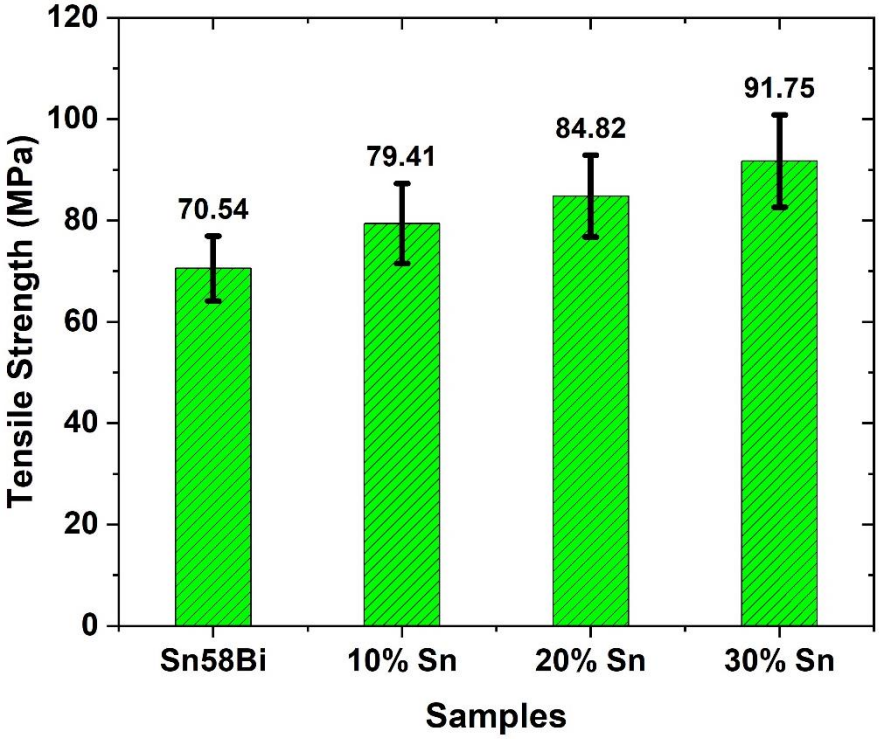

Figure 6 Tensile Strength of Sn58Bi before and after addition of different wt% of Sn particles.

Tables:

Table 1: Stress and Strain values of Sn58Bi solder powder before and after addition of different wt% of Sn particles

Samples	Stress (MPa)	Strain (mm)
Sn58Bi	70.54±6.41	6.11±0.36
Sn58Bi+10%Sn	79.41±7.32	6.33±0.29
Sn58Bi+20%Sn	84.82±8.03	7.03±0.41
Sn58Bi+30%Sn	91.75±8.67	7.96±0.33